

BBA 45542

WAVELENGTH-DEPENDENT QUANTUM YIELDS OF CHLOROPLAST PHOSPHORYLATION CATALYZED BY PHENAZINE METHOSULPHATE

MARTIN SCHWARTZ

Research Institute for Advanced Studies, Baltimore, Md. (U.S.A.)

(Received October 28th, 1966)

SUMMARY

Studies of phenazine methosulphate (PMS)-catalyzed O_2 exchange and phosphorylation in spinach chloroplasts reveal that at short wavelengths ($< 680\text{ m}\mu$) PMS acts at a reduced quantum efficiency as an oxidant for O_2 evolution with concomitant phosphorylation. The quantum yield profile of phosphorylation obtained with PMS differs markedly from the yield profile of phosphorylation for normal chloroplasts with $NADP^+$ or ferricyanide as oxidant. Between 525 and $680\text{ m}\mu$ the quantum yield of phosphorylation (ϕATP) catalyzed by PMS is less than half the constant maximum ϕATP of the normal system. The maximum ϕATP value for the normal system is approx. $0.16\text{ ATP}/h\nu$. With the PMS system a peak in the yield at $690\text{ m}\mu$ is obtained approaching the ϕATP value of the normal system. This yield falls again at longer wavelengths ($> 700\text{ m}\mu$).

The addition of ascorbate to the PMS phosphorylating system decreases the short-wavelength ($< 680\text{ m}\mu$) phosphorylation activity but increases the long-wavelength ($> 690\text{ m}\mu$) phosphorylation activity. The quantum yield profile of this system, showing a long-wavelength rise in phosphorylation efficiency is obtained with or without the addition of 3(3,4-dichlorophenyl)-1,1-dimethylurea.

These experiments have been interpreted as indicating two separate electron-transfer processes catalyzed by PMS, one in which PMS acts at a reduced efficiency as a Hill oxidant, and the other in which PMS acts as an electron donor and acceptor in a cyclic fashion in sensitizing and essentially long-wavelength phosphorylation process.

INTRODUCTION

According to the current series concept of two photoacts in photosynthesis, phosphorylation (ATP synthesis) occurs at a single site concomitant with the oxidation of the weak reductant of photosystem II by the weak oxidant of photosystem I (see refs. 1-3). Phosphorylation catalyzed by phenazine methosulphate (PMS) is considered to occur at the same site concomitant with a recycling of electrons through system I (see refs. 4,5). The action spectrum of phosphorylation for this catalyst should therefore reflect the absorption characteristics of photosystem I. However,

Abbreviations: DCMU, 3(3,4-dichlorophenyl)-1,1-dimethylurea; PMS, phenazine methosulphate.

the action spectrum for PMS-catalyzed phosphorylation obtained by JAGENDORF *et al.*⁶ shows no significant differences from ferricyanide-catalyzed phosphorylation. There is, nevertheless, a report by KOK AND HOCH² showing an increased activity for PMS-catalyzed phosphorylation with dense chloroplast suspensions in 710-m μ actinic light, a wavelength at which NADP⁺ or ferricyanide support poor phosphorylating efficiencies.

This report presents results obtained with spinach chloroplasts which demonstrate that under proper conditions PMS supports phosphorylation at long wavelengths. With this catalyst the quantum yield profile of phosphorylation as a function of wavelength differs markedly from that obtained with the normal, O₂-evolving, Hill reaction system with either ferricyanide or NADP⁺ as oxidant.

METHODS

Chloroplasts were prepared from leaves of several varieties of spinach (*Spinacea oleracea*; varieties Hybrid-22, Virginia Blight, Dixie Market, and America) grown in the greenhouse attached to the Institute. The chloroplasts were prepared in a Tris-sucrose medium as described previously⁷. Total chlorophyll (*a* + *b*) and the ratio of chlorophyll *a* to *b* were determined according to ARNON's procedure⁸.

PMS was purchased from Sigma Biochemical Co., its concentration was determined spectrophotometrically in 0.05 M Tris-HCl (pH 8) at 387.5 m μ employing an $\epsilon_{\text{mM}} = 26.3$ (see ref. 9).

Pyocyanine was prepared from PMS by the method of JAGENDORF AND MARGULIES¹⁰. Its concentration was determined in 0.05 M Tris-HCl (pH 8) at 690 m μ , employing an $\epsilon_{\text{mM}} = 4.5$.

[³²P]P_i was obtained from Oak Ridge National Laboratories, Oak Ridge, Tenn. The isotope was further purified on an anion-exchange resin (chloride form; Bio-Rad, AGI-X8).

ATP synthesis was measured as previously described as the esterification of [³²P]P_i (ref. 7). The [³²P]P_i employed in the assay showed a "break-through" of less than 0.02 % of the total counts.

Polarographic measurements were made with a modified Clark electrode^{7,11}. The sensitivity of the polarographic apparatus was such that one could operate with full-scale deflection equal to a change in O₂ concentration of 9 μ M. The formation of H₂O₂ was determined as O₂ evolution with the polarograph after the addition of catalase^{7,11}.

Fluorescence emission spectra were obtained with the instrument designed in this laboratory by Kok.

Phosphorylation experiments were performed in air at 20° in standard spectrophotometer cuvettes (1-cm light path). In most experiments six cuvettes were exposed simultaneously. Each cuvette was fitted with a vibrating rod which agitated the reaction mixture (2 ml) throughout the exposure time. The optical arrangement was similar to that described by HOCH AND MARTIN¹². The interference filters employed (Thin Films Inc., Cambridge, Mass.) had 5-m μ half-bands and were blocked to infinity on the long-wavelength side of the spectrum and to X-rays on the short-wavelength side.

Absorption measurements of the chloroplast suspensions at various wavelengths

TABLE I

PER CENT ABSORPTION MEASUREMENTS FOR SPINACH CHLOROPLASTS

Kok sphere, 1.0 cm light path.

Wavelength* (mμ)	5 μg Chl _t ** per ml	10 μg Chl _t ** per ml	20 μg Chl _t ** per ml	40 μg Chl _t ** per ml
730	0.49	0.98	1.96	3.90
720	1.23	2.48	4.90	9.53
710	3.06	6.0	11.65	22.0
700	6.77	13.1	24.5	43.0
690	18.4	33.4	55.6	80.3
680	34.5	57.1	81.6	96.6
670	31.55	53.1	78.0	94.2
660	22.2	39.5	63.3	86.6
650	18.95	34.3	56.8	81.3
640	14.65	26.6	46.2	71.0

* Half-band, 5 mμ.

** Chl_t = total chlorophyll (*a* + *b*).

were made with the "Kok" split-beam integrating sphere. The absorption values for the chloroplast suspensions are shown in Table I. When the chloroplast absorption values shown in Table I are converted to absorbance values, one obtains a linear extrapolation of absorbance with chloroplast concentration passing through the origin. The most satisfactory results require appropriate solutions of MgO as the "scatter-blank" for determining the absorption values for the chloroplast suspensions.

In the wavelength region 640–730 mμ corrected absorption values for chloroplast suspensions in the presence of pyocyanine were obtained by employing the "Innere Lichtfilterwirkung" equation of KLING, NIKOLAISKI AND SCHLAFFER¹³,

$$I_{\text{abs.}}(\%) = \frac{A_{\text{chl.}}}{A_{\text{chl.}} + A_{\text{pyo.}}} \left[1 - e^{-2.303 (A_{\text{chl.}} + A_{\text{pyo.}})} \right] \times 100$$

where the absorbance values employed in this calculation are obtained from the integrating-sphere absorption measurements with the various interference filters. The expression $[1 - e^{-2.303 (A_{\text{chl.}} + A_{\text{pyo.}})}]$ is simply the total absorption predicted according to this formula for a combination of the appropriate chloroplast concentration and the appropriate pyocyanine concentration. The total absorption value actually measured in the integrating sphere for the combination of chloroplasts and pyocyanine is consistent with the calculated total absorption value.

Incident light intensities were measured with a bolometer calibrated with a standard lamp as described previously¹⁴. The bolometer calibration was also checked against two other independent calibration standards, (1) the potassium ferrioxalate actinometer¹⁵, and (2) the thermopile of Kok which had been calibrated in Holland.

The unit of intensity employed in this report is the mμEinstein (1 mμmole quanta) per min. The light intensities absorbed by the chloroplasts I_{abs} , were obtained as the multiplication product of the incident intensity and the per cent absorption for the appropriate wavelengths and chlorophyll concentration. Incident intensities were adjusted with calibrated screens for equivalent absorbed intensity at all wavelengths.

The quantum efficiency (yield) of phosphorylation (ϕ ATP) is defined as follows:

$$\phi \text{ ATP} = \frac{\text{ATP molecules formed}}{\text{light quanta absorbed}}$$

All quantum yield determinations were obtained with absorbed light intensities less than 5 % of that required for saturating the system under investigation. Under these conditions and at all wavelengths investigated the actinic intensity could be doubled or halved without affecting the quantum yield values appreciably.

The standard reaction mixture contained the following components in μ moles per 2 ml; Tris-HCl (pH 8), 50; MgCl_2 , 15; NaCl, 35; sucrose 40; ^{32}P -labeled potassium phosphate (containing approx. $3 \cdot 10^6$ counts/min), 3; ADP, 2.5; spinach chloroplasts and other components as indicated in the figures and tables.

RESULTS

Fig. 1 shows the quantum yield profiles of phosphorylation for various types of PMS-mediated chloroplast activity. For comparison, the phosphorylation yield profile is included for the normal (O_2 -evolving) system with NADP^+ as oxidant (Curve 1). The data were obtained from eight or more individual experiments per-

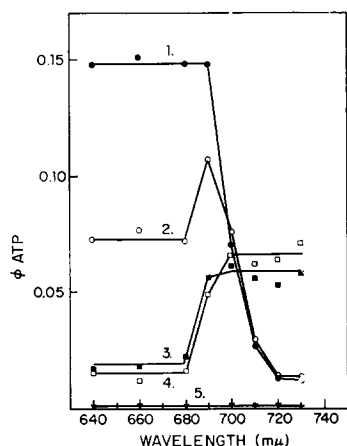


Fig. 1. Wavelength profile of the quantum yield of phosphorylating activity catalyzed by PMS. All vessels contained the reaction mixture as described in the METHODS section. The absorbed intensities were approx. $25 \text{ m}\mu\text{Einstein/min}$ at all wavelengths. The concentration of the various addition reactants were: Curve 1, 1 mM NADP^+ (plus ferredoxin); Curve 2, $20 \mu\text{M}$ PMS; Curve 3, same as Curve 2 plus 10 mM sodium ascorbate; Curve 4, same as Curve 3 plus $2 \mu\text{M}$ DCMU; Curve 5, same as Curve 2 plus $2 \mu\text{M}$ DCMU; and $5 \mu\text{g/ml}$ total chlorophyll. The temperature was 20° and the atmosphere was air.

formed on separate days. Variations between the absolute ϕ ATP values at the respective wavelengths were of the order of 15 %. However, the relative shape of the wavelength-dependent profiles for any individual experiment was essentially invariant.

At short wavelengths ($< 680 \text{ m}\mu$), the quantum yield of PMS-catalyzed phosphorylation (Fig. 1, Curve 2) is less than 50% ϕ ATP for the normal system (Curve 1). The quantum yield profile of PMS-catalyzed phosphorylation attains a maximum near $690 \text{ m}\mu$ and falls at longer wavelengths ($> 700 \text{ m}\mu$). The addition of ascorbate to

the PMS system (Curve 4) suppresses ϕ ATP at short wavelengths ($< 680 \text{ m}\mu$) but increases ϕ ATP at longer wavelengths. Between 710 and $730 \text{ m}\mu$, ϕ ATP is relatively constant and amounts to approx. 40 % of the maximum ϕ ATP of the normal system (Curve 1).

The addition of dichlorodimethylphenylurea (DCMU) does not change the wavelength profile of the ascorbate-PMS system (Curve 3), although at rate-limiting intensities DCMU completely inhibits the phosphorylation mediated by PMS in the absence of ascorbate (Curve 5). Variation of the PMS concentration between 10 and $40 \text{ }\mu\text{M}$, of ascorbate between 2 and 20 mM, and of chloroplasts between 2.5 and $10 \text{ }\mu\text{g}$ total chlorophyll per ml showed no effect on the profiles as presented in Fig. 1. Moreover, the addition of NADP^+ plus ferredoxin to the respective reaction mixtures employed in obtaining Curves 2, 3, and 4 (Fig. 1) did not affect the phosphorylation yield profiles in these systems.

TABLE II

QUANTUM YIELD OF PMS-CATALYZED PHOSPHORYLATION

The reaction mixture is described in the METHODS section. The concentration of the additional reactants were: $20 \text{ }\mu\text{M}$ PMS and 0.75 mM ferricyanide, and spinach chloroplasts containing the respective chlorophyll concentrations as indicated. Temperature, 20° ; atmosphere, air.

Wave-length ($\text{m}\mu$)	Substrate	Chl_t^* ($\mu\text{g/ml}$)	Time (min)	ATP** (μmoles per min)	$I_{\text{abs.}}$ ($\mu\text{Einstein}$ per min)	$\phi \text{ ATP}$ (ATP/quanta)
640	PMS	5	2	2.38	40.3	0.059
640	PMS	5	4	2.26	40.3	0.056
640	PMS	5	2	1.22	21.4	0.057
640	PMS	5	4	1.28	21.4	0.060
640	PMS	10	2	2.15	39.9	0.054
640	PMS	10	4	2.15	39.9	0.054
640	$\text{Fe}(\text{CN})_6^{3-}$	5	2	3.07	21.4	0.144
640	$\text{Fe}(\text{CN})_6^{3-}$	10	2	5.43	39.9	0.136
690	PMS	5	2	4.00	36.7	0.109
690	PMS	5	4	3.78	36.7	0.103
690	PMS	5	2	1.97	19.5	0.101
690	PMS	5	4	2.11	19.5	0.108
690	$\text{Fe}(\text{CN})_6^{3-}$	5	2	4.51	36.7	0.123
690	$\text{Fe}(\text{CN})_6^{3-}$	5	4	2.52	19.5	0.129

* Chl_t = total chlorophyll ($a + b$).

** Dark controls showed 0.019 % of total counts. The ATP rates are the corrected values.

Under our experimental conditions the quantum yield profiles of the PMS or ferricyanide systems (Table II) are not affected by the "phosphorylation lag" reported by SHEN AND SHEN¹⁶, since essentially constant ϕ ATP values are obtained with variation of light intensity, chloroplast density and duration of experiment. According to the data of SHEN AND SHEN¹⁶ the pool size responsible for the phosphorylation lag expressed as ATP:total chlorophyll is of the order of 1:20. With our experimental procedure and under the most extreme conditions of low actinic light intensity, chlorophyll concentration, and duration of experiment, the lowest ratio of ATP formed to chlorophyll concentration was 1:5. Consequently, the phosphory-

lation data in this report would not be significantly affected by the existence of such a lag.

The various PMS-mediated chloroplast activities also include its catalytic participation in ferricytochrome *c* reduction. DAVENPORT¹⁷, and KEISTER AND SAN PIETRO¹⁸ demonstrated with chloroplasts that PMS acts as a catalyst for ferricytochrome *c* reduction and converts PMS-catalyzed electron transport into a normal O₂-evolving system. The data in Table III show that with added cytochrome *c* at

TABLE III

COMPARISON OF QUANTUM YIELDS FOR PMS-CATALYZED PHOSPHORYLATION ACTIVITY UNDER VARIOUS CONDITIONS

Reaction mixture as described in METHODS section. Temperature, 20°; atmosphere, air; reaction time, 4 min; total chlorophyll, 5 µg/ml; *I*_{abs.}, 29.4 mµEinstein/min; wavelength, 640 mµ.

Substrate (µmole/2.0 ml)	ATP formed (mµmoles/min)	φ ATP (ATP/quantum)
NADP ⁺ , 0.1; (c ferredoxin)	4.17	0.142*
NADP ⁺ , 0.1	0.08	0.003
PMS, 0.04; cytochrome <i>c</i> , 0.2	4.44	0.151*
PMS, 0.04	1.87	0.064
PMS, 0.04; NADP ⁺ , 0.1; (c ferredoxin)**	1.81	0.062
PMS, 0.04; ascorbate, 10	0.64	0.022
Cytochrome <i>c</i> , 0.2	0.13	0.004
Cytochrome <i>c</i> , 0.2 (c ferredoxin)	4.21	0.143

* Corresponding measurements of the quantum yields of NADP⁺ reduction and ferricytochrome *c* reduction yielded P/2e ratios approaching unity.

** The concentration of ferredoxin could be increased 4-fold without an apparent effect on φ ATP.

short wavelengths (*i.e.* 640 mµ) PMS mediates an efficient normal phosphorylating system. Thus, the decreased φ ATP values obtained at short wavelengths (*i.e.* 640 mµ) with PMS alone are not attributable to a limited availability of the concentration of oxidized PMS. Moreover, the addition of NADP⁺ plus ferredoxin to the PMS phosphorylating system did not affect φ ATP (Table III). The availability of NADP⁺ as an oxidant for the low-potential reductant formed in the light should change the φ ATP values if, indeed, the phosphorylation rates were limited by the concentration of oxidized PMS. Comparable φ ATP results (Table III) were obtained with the PMS–ferricytochrome *c* couple, the ferredoxin–ferricytochrome *c* couple, and the ferredoxin–NADP⁺ couple, suggesting that oxidized PMS and ferredoxin react with the same low-potential reductant. Taken together, the data in Table III and Fig. 1 indicate that the control of PMS-catalyzed phosphorylation depends on the electron-donor (reductant) activity of PMS.

The most generally accepted hypothesis for interpreting the reductant activity of PMS requires that reduced PMS acts as an electron donor at some site in the electron-transport chain between the two photosystems⁵. One, therefore, expects the wavelength profile of φ ATP to resemble the photochemical activity of photosystem I. That PMS activity also involves photosystem II has generally been excluded because previously only low rates of O₂ exchange were observed concomitant with high rates

TABLE IV

PMS-CATALYZED O_2 PRODUCTION AND CONSUMPTION

Reaction mixture as described in METHODS section. Temperature, 20°; volume, 1.2 ml; total chlorophyll, 5 $\mu\text{g/ml}$; I_{abs} at 640 $m\mu$, 41.4 $m\mu\text{Einstein/min}$; I_{abs} at 690 $m\mu$, 35.1 $m\mu\text{Einstein/min}$.

Wavelength ($m\mu$)	Reagent ($\mu\text{mole/ml}$)	+ O_2 ($m\mu\text{moles/min}$)	- O_2 ($m\mu\text{moles/min}$)	H_2O_2 formed* ($m\mu\text{moles/min}$)
640	Fe(CN)_6^{3-} , 0.6	+3.28	—	± 0
640	Methyl viologen, 0.05	—	-3.39	+6.70
640	PMS, 0.02	—	-1.03	+2.30
640	PMS, 0.02; DCMU, 0.002	± 0	± 0	± 0
640	No additions	—	<0.05	<0.10
690	Fe(CN)_6^{3-} , 0.6	+2.57	—	± 0
690	PMS, 0.02	—	-0.95	+2.06
690	Methyl viologen, 0.05	—	-2.48	+5.10
690	PMS, 0.02; DCMU, 0.002	± 0	± 0	± 0

* H_2O_2 formation was determined as O_2 production after a 7-min reaction period by the addition of 0.01 ml of a solution of catalase, where $H_2O_2 \xrightarrow{\text{catalase}} H_2O + 1/2 O_2$.

of phosphorylation¹⁹. Nevertheless, we have observed considerable rates of PMS-catalyzed O_2 exchange at low intensities of actinic light. Table IV presents results of polarographic observations of PMS-catalyzed O_2 exchange (as measured by O_2 consumption and H_2O_2 production) with rate-limiting intensities of 640- and 690- $m\mu$ actinic light. The results show that PMS catalyzes a true O_2 evolution indicated by the ratio of H_2O_2 formed to O_2 consumed ($H_2O_2:O_2$ approx. 2). The quantum yield of O_2 production in this reaction is approx. 35 % as efficient as O_2 production catalyzed by ferricyanide. This conclusion regarding O_2 evolution is also supported by the observation that the inhibitor, DCMU, completely blocks PMS-catalyzed O_2 consumption and H_2O_2 formation. The O_2 -exchange data suggest that at low intensities in short-wavelength light, PMS-catalyzed phosphorylation is mainly coupled to

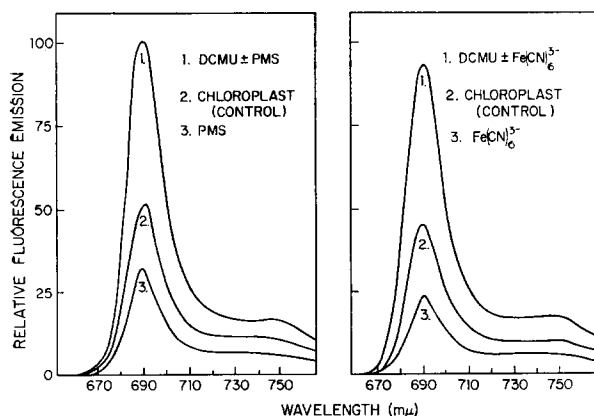


Fig. 2. Quenching of chloroplast fluorescence. Reaction mixture and conditions as described previously. The total chlorophyll concentration was 10 $\mu\text{g/ml}$. The intensity of the exciting light (578 $m\mu$) was rate-limiting. The concentration of the additional reactants were: 20 μM PMS; 0.75 mM ferricyanide; 2 μM DCMU. The temperature was 20° and the atmosphere was air.

the O_2 -evolving activity of PMS. Why this activity of PMS is less efficient than that of ferricyanide or of methyl viologen (Table IV) is not clear. In any case, it must be related to a competition between the reductant activity of PMS and water as an electron donor.

Fluorescence emission measurements with chloroplasts (Fig. 2) suggest that the reductant activity of PMS involves, in part, a site of entry into the chloroplast electron-transport chain in photosystem II. According to DUYSSENS AND SWEERS²⁰, the quenching of the 690-m μ fluorescence emission of chloroplasts depends on an operational electron transport through photosystem II. The steady-state fluorescence emission curves (Fig. 2) show that at rate-limiting intensities of actinic light, 20 μ M PMS quenches fluorescence to approximately the same extent as ferricyanide. The quenching of fluorescence by PMS and ferricyanide is abolished by DCMU. Accordingly, a site of PMS reductant activity in photosystem II is indicated.

Finally, pyocyanine, an oxidation product of PMS reported by HILL AND WALKER²¹ to be an effective catalyst of phosphorylation was assayed under our conditions. Fig. 3 shows the quantum yield profile of phosphorylation mediated by pyocyanine. As in Fig. 1, the ϕ ATP profile mediated by $NADP^+$ is included for

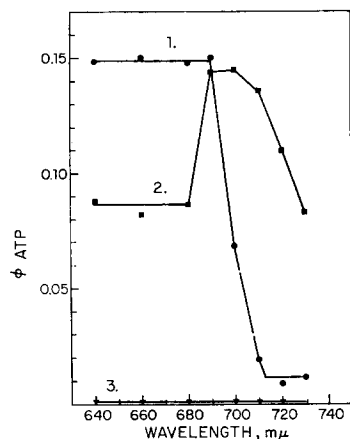


Fig. 3. Wavelength profile of the quantum yield of pyocyanine-catalyzed phosphorylation. All vessels contain the standard reaction mixture as described in the METHODS section. The absorbed intensities were approx. 25 m μ Einstein/min at all wavelengths. The concentration of the additional reactants were: Curve 1, 1 mM $NADP^+$ (plus ferredoxin); Curve 2, 25 μ M pyocyanine; Curve 3, same as Curve 2 plus 2 μ M DCMU and 5 μ g/ml chlorophyll.

reference (Curve 1). The pyocyanine data were obtained from averages of four independent experiments. It can be seen from Fig. 3, Curve 2, that pyocyanine-mediated phosphorylation also shows an active long-wavelength phosphorylation process. At short wavelengths (< 680 m μ) pyocyanine-catalyzed phosphorylation is suppressed with respect to the normal, O_2 -evolving phosphorylation system. The differences between the quantum yield profiles for PMS and pyocyanine are manifested principally at long wavelengths (> 690 m μ). In 700-m μ actinic light pyocyanine remains an efficient cofactor of phosphorylation falling gradually to lower efficiencies at longer wavelengths. At all wavelengths of actinic light DCMU completely inhibits the pyocyanine-mediated phosphorylation system (Curve 3). The addition of ascorbate

does not reverse the inhibition of phosphorylation by DCMU as one might predict since pyocyanine (E_0' approx. -0.03 V) is not reduced by ascorbate (E_0' approx. 0.0 V).

DISCUSSION

The results reported above indicate that PMS acts at short wavelengths as a Hill oxidant and as an electron donor for chloroplasts at long wavelengths. The data require that at short wavelengths (< 680 m μ), phosphorylation catalyzed by PMS result principally from its activity as a Hill oxidant. That is, at short wavelengths phosphorylation observed with PMS (Fig. 1) is essentially the normal, O_2 -evolving phosphorylation system operating at a decreased efficiency (approx. 35 %) as indicated by the O_2 -exchange data (Table IV). Phosphorylation with the PMS-ferri-cytochrome *c* couple (Table III) shows that PMS maintained in its oxidized state, and thereby prevented from recycling, catalyzes the normal type of phosphorylation in short-wavelength light.

The data (Fig. 1 and Table III) also show that reduced PMS increases the long-wavelength phosphorylation activity and decreases the short-wavelength phosphorylation activity. The addition of NADP *plus* ferredoxin does not affect these results. Accordingly, the quantum yield profile of phosphorylation obtained with PMS as a catalyst showing a peak at 690 m μ (Fig. 1, Curve 2) can be visualized as the combined activity of two photosensitized electron-transfer processes. In the first, PMS acts at short wavelengths with a reduced efficiency as a Hill oxidant, and in the other PMS acts in a cyclic fashion as an electron donor and acceptor in sensitizing a long-wavelength phosphorylation process. Thus, the peak in ϕ ATP at 690 m μ is the net result of an overlap of these two phosphorylating systems. Thus, net phosphorylation increases at 690 m μ because of the onset of the long-wavelength phosphorylation activity of reduced PMS (Fig. 1, Curves 3 and 4). At longer wavelengths (> 690 m μ) the PMS phosphorylation system associated with O_2 evolution decreases. A corresponding decrease in the long-wavelength phosphorylation process also occurs which is probably the result of the limited concentration of reduced PMS. The net result is observed as a decrease in PMS-catalyzed phosphorylation at wavelengths longer than 690 m μ when compared with the ascorbate-PMS system (Fig. 1). If this interpretation of the long-wavelength drop in PMS-catalyzed phosphorylation is correct, one might expect that at higher light intensities the maximum of the phosphorylation profile for PMS would shift to longer wavelengths because the concentration of reduced PMS would be increased. The PMS phosphorylation profile measured at high light intensities by KOK AND HOCH² shows such a shift to longer wavelengths.

The quantum yield profile obtained with pyocyanine (Fig. 3, Curve 2) shows a far more pronounced long-wavelength stimulation of the quantum yield of phosphorylation than the PMS phosphorylation profile. However, the phosphorylation results obtained with the two catalysts are qualitatively similar, indicating that the same general interpretation can apply for the activity of both catalysts.

A possible interpretation of the fluorescence data obtained with PMS (Fig. 2) and the low ϕ ATP values obtained at short wavelengths (< 690 m μ) with the ascorbate-PMS couple is that in short-wavelength light one site of entry of electrons donated by reduced PMS occurs in photosystem II. This electron-donor activity of

PMS is not associated with phosphorylation since the yield of phosphorylation at short wavelengths can be accounted for by the Hill oxidant activity of PMS (P/O approx. 1.3). The decreased O_2 -evolving activity could be the result of this electron-donor activity. If this interpretation is correct, the existence of a phosphorylation site between photoacts is excluded since little or no phosphorylation activity is associated with this reductant activity of PMS.

Additional sites of entry of electrons into the chloroplasts are required for interpreting the phosphorylation data obtained at long wavelengths ($> 690\text{ m}\mu$) with the ascorbate-PMS couple in DCMU-poisoned chloroplasts. At least two sites of entry of electrons subsequent to photosystem II are required to account for the poor long-wavelength ϕATP (compared to the normal system in short wavelengths) catalyzed by the ascorbate-PMS couple. The existence of parallel pathways of electron-donor activity in chloroplasts is indicated by the observation of KOK, RURAISKI AND HARMON²² showing that reduced plastocyanine and ferredoxin *f* operate in parallel and not in series in catalyzing system I-type reactions. Fig. 4 represents this proposal for the electron-flow sequence involved in PMS catalysis as described above.

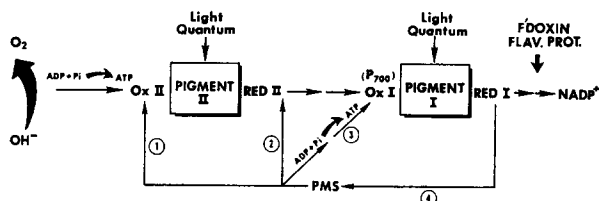


Fig. 4. Proposed mechanism for the oxidant and reductant activity of PMS. (1) Reductant activity of PMS without concomitant phosphorylation in short-wavelength light derived from fluorescence emission data (Fig. 2) and poor quantum yield of phosphorylation (Fig. 1 and Tables II and III). (2) Reductant activity of PMS without concomitant phosphorylation in long-wavelength light. This site of reductant activity is required to account for the relatively poor yields of phosphorylation catalyzed by the PMS-ascorbate couple (Fig. 1). (3) Reductant activity of PMS with concomitant phosphorylation in long-wavelength light. This site is required to account for the phosphorylation observed with the ascorbate-PMS couple in the presence of DCMU. The data and interpretations require that this phosphorylation site be separated from the main electron-transport chain (see discussion). (4) Oxidant activity of PMS. The data (Table III) suggests that PMS reacts as an oxidant with the same low-potential reductant as ferredoxin.

Future experiments may modify the proposal (Fig. 4) offered for explaining the activity of PMS in chloroplast phosphorylation. However, what is clearly indicated by the data is the presence in chloroplasts of a short-wavelength-sensitized phosphorylation process and a long-wavelength-sensitized phosphorylation process. That this activity represents the action of more than one site of phosphorylation associated with the electron-transport activity of chloroplasts is only suggested as an interpretation of the data reported above. The fact that the maximum ϕATP values obtained in the normal system are never exceeded by PMS or pyocyanine catalysis is troublesome since one would expect that under proper conditions the operation of more than a single site of phosphorylation should yield high ϕATP values.

ACKNOWLEDGEMENTS

This work was supported in part by a contract with the Office of Naval Research, Nonr-4753(00).

I wish to express my thanks to Mr. G. A. EBERT for his excellent assistance and also to Dr. B. KOK for his thought-provoking comments and discussions throughout the course of this investigation.

REFERENCES

- 1 R. HILL AND F. BENDALL, *Nature*, 186 (1960) 136.
- 2 B. KOK AND G. HOCH, in W. D. McELROY AND B. GLASS, *Light and Life*, Johns Hopkins, Baltimore, 1961, p. 397.
- 3 L. N. M. DUYSSENS, J. AMESZ AND B. M. KAMP, *Nature*, 190 (1961) 510.
- 4 A. T. JAGENDORF AND M. AVRON, *J. Biol. Chem.*, 231 (1958) 277.
- 5 D. I. ARNON, M. LOSADA, F. R. WHATLEY, H. Y. TSUJIMOTO, D. O. HALL AND A. A. HORTON, *Proc. Natl. Acad. Sci. U.S.*, 47 (1961) 1314.
- 6 A. T. JAGENDORF, S. B. HENDRICKS, M. AVRON AND M. B. EVANS, *Plant Physiol.*, 33 (1958) 72.
- 7 M. SCHWARTZ, *Biochim. Biophys. Acta*, 112 (1966) 204.
- 8 D. I. ARNON, *Plant Physiol.*, 24 (1949) 1.
- 9 W. S. ZAUGG, *J. Biol. Chem.*, 239 (1964) 3964.
- 10 A. T. JAGENDORF AND M. MARGULIES, *Arch. Biochem. Biophys.*, 90 (1960) 184.
- 11 M. SCHWARTZ, *Biochim. Biophys. Acta*, 102 (1964) 361.
- 12 G. HOCH AND I. MARTIN, *Arch. Biochem. Biophys.*, 102 (1963) 430.
- 13 O. KLING, E. NIKOLAISKI AND H. L. SCHLAFFER, *Ber. Bunsenges. Physik. Chem.*, 67 (1963) 883.
- 14 M. SCHWARTZ, *Arch. Biochem. Biophys.*, 59 (1955) 5.
- 15 C. G. HATCHARD AND C. A. PARKER, *Proc. Roy. Soc. London, Ser. A*, 235 (1956) 518.
- 16 Y. K. SHEN AND G. M. SHEN, *Sci. Sinica Peking*, 11 (1962) 1097.
- 17 H. E. DAVENPORT, *Proc. Roy. Soc. London, Ser. B*, 157 (1963) 332.
- 18 D. L. KEISTER AND A. SAN PIETRO, *Arch. Biochem. Biophys.*, 103 (1963) 45.
- 19 A. R. KRALL, N. E. GOOD AND B. C. MAYNE, *Plant Physiol.*, 36 (1961) 44.
- 20 L. N. M. DUYSSENS AND H. E. SWEERS, *Studies on Microalgae and Photosynthetic Bacteria*, Univ. of Tokyo Press, Tokyo, 1963, p. 353.
- 21 R. HILL AND D. A. WALKER, *Plant Physiol.*, 34 (1959) 240.
- 22 B. KOK, H. J. RURAINSKI AND E. A. HARMON, *Plant Physiol.*, 39 (1964) 513.

Biochim. Biophys. Acta, 131 (1967) 548-558